Triple shape coexistence and shape evolution in the $N = 58$ Sr and Zr isotopes

A. Petrovici*

National Institute for Physics and Nuclear Engineering - Horia Hulubei, R-077125 Bucharest, Romania

(Received 20 January 2012; revised manuscript received 14 March 2012; published 30 March 2012)

The triple shape coexistence specific for the 0^+ states and the evolution of the shape coexistence and mixing in the neutron-rich $N = 58$ Sr and Zr isotopes are studied within the *complex* excited VAMPIR approach using a realistic effective interaction based on the Bonn A potential in a large model space. The influence of the shape mixing on the structure and dynamics of the positive-parity states up to spin 20^+ in ^{96}Sr and ^{98}Zr is discussed and comparison to the available data is presented.

DOI: 10.1103/PhysRevC.85.034337 PACS number(s): 27.60.+j, 21.60.−n, 21.10.−k

I. INTRODUCTION

The investigation of the neutron-rich nuclei in the $A \simeq 100$ mass region is receiving an increasing interest both theoretically and experimentally. The structure of these nuclei relevant for the astrophysical r-process manifests drastic changes in some isotopic chains and often sudden variations of particular nuclear properties have been identified. Neutron-rich Sr and Zr nuclei indicate rapid transition from spherical to deformed shape with a possible identification of the sudden onset of quadrupole deformation increasing the neutron number from $N = 58$ to $N = 60$ [1–10]. Previous theoretical investigations revealed the difficulty of describing the shape coexistence and shape transition suggested by the experimental data at low spins and the richness of various structural effects occurring at intermediate and high spins.

As the best examples of nuclei manifesting shape coexistence in the region, Sr and Zr nuclei around $N = 58$ were studied within different theoretical models including the generator coordinate method (GCM) [11], the macroscopic-microscopic method [12], the shell model [13–16], the Monte Carlo shell model [17], the interacting boson model (IBM) approximation [18], the Hartree-Fock (HF) and Hartree-Fock-Bogoliubov (HFB) models [13,19], the VAMPIR model [20,21], and covariant density functional (DF) theory [22]. For a realistic description of the evolution in structure with increasing energy, spin, and isospin determined by shape coexistence and mixing beyond-mean-field approaches are required.

The present study is an attempt at a self-consistent description of the shape coexistence phenomena in the neutron-rich Sr and Zr isotopes at the critical number of neutrons $N = 58$. Since the onset of deformation is supposed to take place for $N > 58$ we investigated the structural changes and the evolution of deformation with increasing spin, aiming at a unitary description of the lowest few 0^+ states and the low, intermediate, and high spins in ^{96}Sr and ^{98}Zr. In this work the properties of the positive-parity states up to spin 20^+ in ^{96}Sr and ^{98}Zr are studied within the *complex* excited VAMPIR variational model with symmetry projection before variation using a realistic effective interaction and a large model space.

In the next section the *complex* excited VAMPIR variational procedure will be briefly described and the effective Hamiltonian will be defined. In Sec. III the results concerning the shape coexistence phenomena specific for the lowest 0^+ states as well as the lowest positive-parity bands in ^{96}Sr and ^{98}Zr will be discussed. Finally, some conclusions will be presented in Sec. IV.

II. THEORETICAL FRAMEWORK

The *complex* excited VAMPIR model uses Hartree-Fock-Bogoliubov (HFB) vacua as basic building blocks which are only restricted by time-reversal and axial symmetry. The underlying HFB transformations are essentially *complex* and do mix proton with neutron states as well as states of different parity and angular momentum. The broken symmetries (nucleon numbers, parity, total angular momentum) are restored by projection techniques and the resulting symmetry-projected configurations are used as test wave functions in chains of successive variational calculations to determine the underlying HFB transformations as well as the configuration mixing. The HFB vacua account for arbitrary two-nucleon correlations and thus simultaneously describe like-nucleon as well as isovector and isoscalar proton-neutron pairing. Furthermore, the *complex* excited VAMPIR model (EXVAM) allows the use of rather large model spaces and realistic effective interactions.

For nuclei in the $A \simeq 100$ mass region is used a rather large model space above the ^{40}Ca core built out of $1p_{1/2}$, $1p_{3/2}$, $0f_{5/2}$, $0f_{7/2}$, $2s_{1/2}$, $1d_{3/2}$, $1d_{5/2}$, $0g_{7/2}$, $0g_{9/2}$, and $0h_{11/2}$ oscillator orbits for both protons and neutrons in the valence space. The corresponding single-particle energies (in units of the oscillator energy $\hbar\omega$) are 0.037, −0.173, 0.299, −1.090, 0.715, 0.932, 0.198, 1.524, 0.034, and 1.186 for the proton, and −0.141, −0.292, 0.038, −1.220, 0.909, 1.044, 0.758, 1.384, −0.038, and 0.873 for the neutron levels, respectively. The single-particle energies had been adjusted in *complex* monster (VAMPIR) calculations [23] for odd-mass nuclei in the $A \simeq 100$ mass region. This rather large model space allows the realistic description of the Gamow-Teller β decay of neutron-rich nuclei in this region [21].

The effective two-body interaction is constructed from a nuclear matter G matrix based on the Bonn A potential. In order to enhance the pairing properties the G matrix was modified by three short-range (0.707 fm) Gaussians for the isospin $T = 1$ proton-proton, neutron-neutron, and neutron-proton matrix elements with strengths of −40, −30, and −35 MeV,

*spetro@nipne.ro

respectively. The isoscalar spin 0 and 1 particle-particle matrix elements are enhanced by an additional Gaussian with the same range and the strength of -70 MeV. In addition the isoscalar interaction was modified by monopole shifts of -0.275 MeV for all $T = 0$ matrix elements of the form $\langle 0g_{9/2}0f; IT = 0|\hat{G}|0g_{9/2}0f; IT = 0\rangle$ involving protons and neutrons occupying the $0f_{5/2}$ and the $0f_{7/2}$ orbitals. The Coulomb interaction between the valence protons was added.

We calculated the lowest positive-parity states up to spin 20^+ in ^{96}Sr and ^{98}Zr including in the excited VAMPIR many-nucleon bases up to 12 EXVAM configurations. The final solutions for each spin have been obtained diagonalizing the residual interaction between the considered excited VAMPIR configurations. For each nucleus the calculated states have been organized in bands based on the $B(E2; \Delta I = 2)$ values connecting them.

III. RESULTS AND DISCUSSION

The theoretical lowest bands of ^{96}Sr and ^{98}Zr are compared to the experimental spectra in Figs. 1 and 2, respectively. The labels of the bands indicate the prolate p or oblate o intrinsic quadrupole deformation for the dominant projected EXVAM configurations underlying the states of the corresponding bands. The states building the po(p) band in each nucleus are characterized by strong prolate-oblate mixing at low spins and variable prolate mixing at intermediate and high spins. The almost pure oblate states belonging to the rightmost band in the theoretical spectrum are feeding the second 4^+ (2^+) state in ^{96}Sr (^{98}Zr) that manifests maximum o-p mixing.

The results concerning the oblate-prolate mixing in the structure of the wave functions for the lowest two 2^+ and 4^+ states is illustrated in Table I. We indicate the contribution of the EXVAM configurations bringing at least 1% of the total

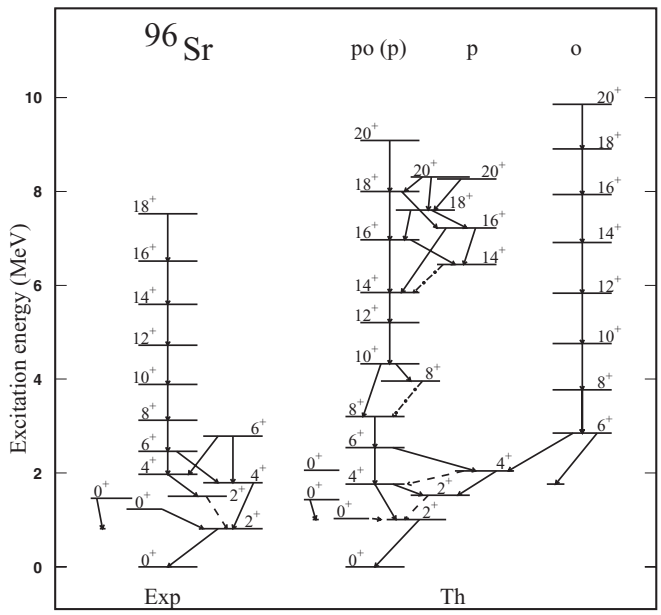

FIG. 1. Theoretical EXVAM spectrum of ^{96}Sr compared to experimental data [3,5,8].

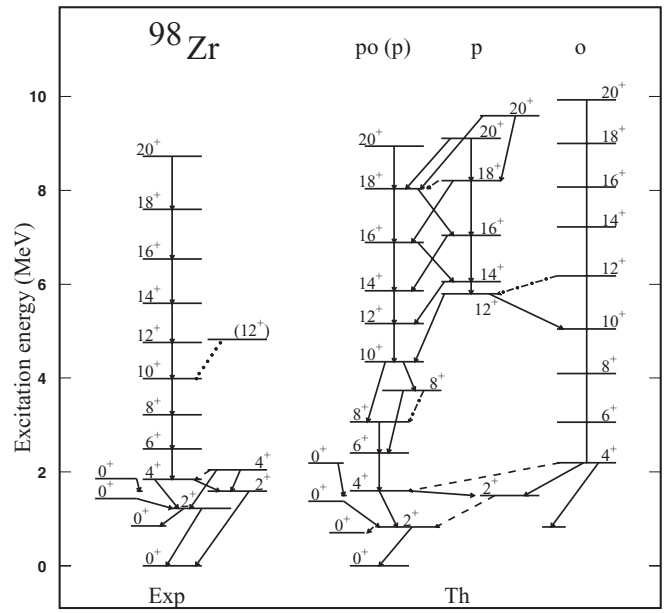

FIG. 2. Theoretical EXVAM spectrum of ^{98}Zr compared to experimental data [3,5,8].

amplitude. In ^{96}Sr the lowest 2^+ configuration is intrinsically oblate deformed, being separated from the first prolate one orthogonal on it by 24 keV. The lowest two orthogonal 4^+ EXVAM configurations are separated by 154 keV but the prolate one is the deepest. In ^{98}Zr the lowest EXVAM configuration is prolate deformed in the intrinsic system for the spin $I^\pi = 2^+$ as well as for 4^+ being separated from the lowest oblate one by 206 and 431 keV, respectively. Recent experimental results give support to the theoretical o-p mixing: the spectroscopic quadrupole moment of the 2_1^+ state in ^{96}Sr is equal to 0 [10] while the calculated value is $Q^{\text{spec}}(2_1^+) = 9.5efm^2$ using the effective charges $e_p = 1.3$ and $e_n = 0.3$. Also the EXVAM results reveal significant $B(E2; \Delta I = 0)$ values for the transitions connecting the lowest 2^+ and 4^+ states: $B(E2; 2_2^+ \rightarrow 2_1^+) = 1712e^2fm^4$, $B(E2; 4_2^+ \rightarrow 4_1^+) = 1120e^2fm^4$ in ^{96}Sr, and $B(E2; 2_2^+ \rightarrow 2_1^+) = 1876e^2fm^4$, $B(E2; 4_2^+ \rightarrow 4_1^+) = 784e^2fm^4$ in ^{98}Zr. Experimentally, a lower limit is available in ^{96}Sr: $B(E2; 2_2^+ \rightarrow 2_1^+) > 232e^2fm^4$ [24]. The mixing specific for the 2^+ and 4^+ states is also responsible for the $E2$ branches decaying the lowest 4^+ states. In ^{96}Sr the calculated strengths are $B(E2; 4_1^+ \rightarrow 2_1^+(2_2^+)) = [1776\,(187)]e^2fm^4$ and $B(E2; 4_2^+ \rightarrow 2_2^+) = 1901e^2fm^4$, while in ^{98}Zr we obtained $B(E2; 4_1^+ \rightarrow 2_1^+(2_2^+)) = [2072\,(620)]e^2fm^4$ and $B(E2; 4_2^+ \rightarrow 2_2^+(2_1^+)) = [1593\,(56)]e^2fm^4$.

TABLE I. The o-p mixing of lowest 2^+ and 4^+ states.

I[$\hbar$]	^{96}Sr		^{98}Zr	
	o mixing	p mixing	o mixing	p mixing
2_1^+	58 (5)%	34 (2)%	31%	60 (8)%
2_2^+	33 (2)%	65%	63 (1)%	36%
4_1^+	36 (6)%	56 (1)%	10%	83 (7)%
4_2^+	52 (5)%	43%	85 (1)%	13 (1)%

TABLE II. Structure of wave functions for lowest four 0^+ states.

$I[\hbar]$	^{96}Sr			^{98}Zr		
	Spherical	Prolate	Oblate	Spherical	Prolate	Oblate
0_1^+	36%	20%	44%	12%	43%	45%
0_2^+	57%	18%	25%	84%	12%	4%
0_3^+		69%	31%	1%	57%	42%
0_4^+	4%	6%	90%	2%	10%	88%

A particular situation is found for the 0^+ states: the lowest-projected EXVAM configuration is spherical in both nuclei (the quadrupole deformation parameter amounts to $\beta_2 \simeq 0.03$). In ^{96}Sr the second 0^+ configuration is oblate deformed in the intrinsic system ($\beta_2 = -0.32$), the third one is prolate ($\beta_2 = 0.37$) and all three orthogonal configurations are situated in an energy interval of 375 keV. In ^{98}Zr the second configuration is prolate ($\beta_2 = 0.37$), the third is oblate ($\beta_2 = -0.30$) and the separation energy between the spherical one and the third one is 323 keV. For each nucleus we constructed the lowest 10 0^+ orthogonal EXVAM configurations and the result of the diagonalization of the residual interaction between them in terms of spherical, prolate, and oblate content is presented in Table II. The structure of the wave functions indicates that the ground state is dominated by oblate components in ^{96}Sr while in ^{98}Zr the oblate and prolate configurations bring a similar contribution. The spherical configuration is distributed over a few states with maximum amplitude in the structure of the first excited 0^+. The third 0^+ state is dominated by different prolate components and the fourth one by oblate components in both nuclei. It is worthwhile to mention that, for both nuclei, a spherical configuration for the spin 2^+ was not found up to 4 MeV excitation energy. In Figs. 3 and 4 we present the occupation of valence single-particle orbitals for the spherical 0^+ EXVAM configuration (the first state in the row for each nucleus) and for the lowest four 0^+ states in ^{96}Sr and ^{98}Zr, respectively. The occupation of the $1d_{5/2}$ neutron

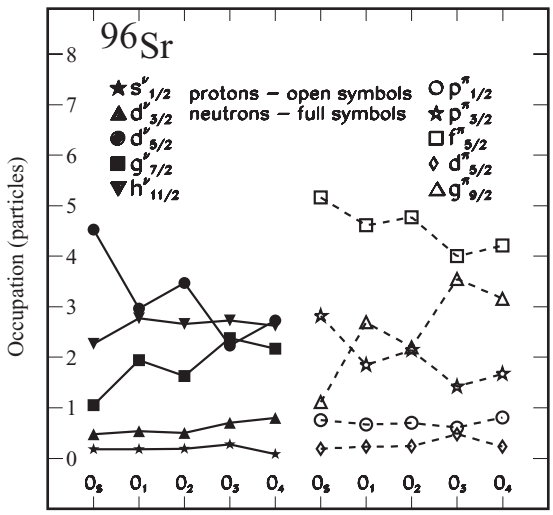

FIG. 3. Occupation of valence spherical orbitals for 0^+ states in ^{96}Sr (see text for explanations).

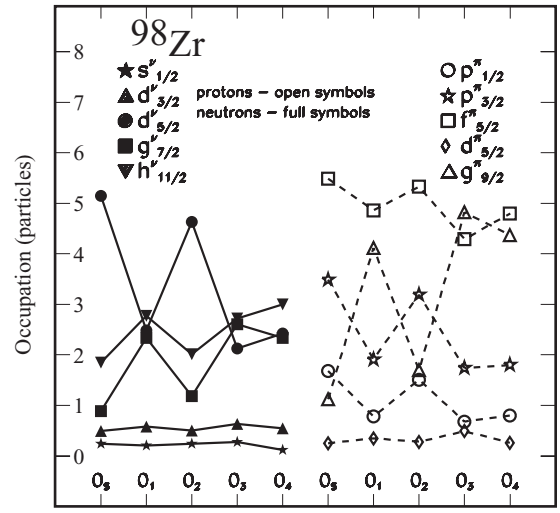

FIG. 4. Same as in Fig. 3, but for ^{98}Zr.

orbital is essential for the spherical 0^+ EXVAM configuration. The occupation of the $0g_{9/2}$ proton orbital is significantly changing from the intrinsically oblate deformed configurations to the prolate deformed ones in both nuclei.

The experimental $B(E2)$ values for the transitions connecting the lowest 0^+ and 2^+ states in ^{96}Sr support the idea of strong shape mixing. The retardation of the $2_1^+ \rightarrow 0_1^+$ transition is induced from the strength $B(E2) = [340\,(209)]e^2fm^4$ deduced from the measured lifetime of 7 (4) ps [2]. Recently, reported results indicate for this lifetime 4.1 ps [10]. The EXVAM strengths connecting the lowest 2^+ and 0^+ states for the two isotopes are compared in Table III. The available data are also presented.

Support for the mixing of configurations with different intrinsic deformations in the structure of the wave functions for the 0^+ states is offered by the strong $\rho^2(E0)$ values found in both nuclei (1, 3, and Nuclear Data Sheets). The EXVAM results reveal also strong $\rho^2(E0)$ values. In Table IV the EXVAM results are compared to the available data. The EXVAM strength $\rho^2(0_3^+ \rightarrow 0_2^+)$ in ^{96}Sr is negligible and there is a cancellation effect between proton and neutron contributions. Since the lowest-three orthogonal EXVAM configurations are very close in energy in both nuclei, a small change in their relative position could change their mixing in the wave functions and the $E0$ strengths connecting them.

TABLE III. $B(E2)$ values (in e^2fm^4) connecting the lowest 2^+ and 0^+ states.

Transition	^{96}Sr		^{98}Zr	
	EXVAM	Expt [2,8,24]	EXVAM	Expt [8,25]
$B(E2; 2_1^+ \rightarrow 0_1^+)$	795	340 (209)	1140	
$B(E2; 0_2^+ \rightarrow 2_1^+)$	2165	400 (42)	990	>30
$B(E2; 0_3^+ \rightarrow 2_1^+)$	110	1 (1)	805	1369 (134)
$B(E2; 0_4^+ \rightarrow 2_1^+)$			2	3 (1)
$B(E2; 0_4^+ \rightarrow 2_2^+)$			140	1181 (107)
$B(E2; 2_2^+ \rightarrow 0_3^+)$	1439		1305	

TABLE IV. $\rho^2(E0)$ values connecting the lowest 0^+ states.

Transition	^{96}Sr		^{98}Zr	
	EXVAM	Expt	EXVAM	Expt
$\rho^2(E0; 0_2^+ \to 0_1^+)$	0.066		0.060	0.012 (1)
$\rho^2(E0; 0_3^+ \to 0_1^+)$			0.001	$\leqslant$0.015
$\rho^2(E0; 0_3^+ \to 0_2^+)$	0.000	0.180	0.012	0.075 (8)
$\rho^2(E0; 0_4^+ \to 0_1^+)$			0.003	$\leqslant$0.010
$\rho^2(E0; 0_4^+ \to 0_2^+)$	0.009		0.019	$\leqslant$0.028
$\rho^2(E0; 0_4^+ \to 0_3^+)$			0.003	0.056 (12)

This problem will be carefully investigated in the future and correlated with expected new data [10].

At intermediate and high spins, specific aspects of shape coexistence and mixing have been identified. For the $I^\pi \geqslant 6^+$ states the lowest EXVAM configuration is prolate deformed in both nuclei. In ^{96}Sr the oblate-prolate mixing is still present (below 8%) for the lowest 6^+ and 8^+ states while for $I^\pi \geqslant 10^+$ the states of the po(p) band manifest a strong mixing of differently deformed prolate EXVAM configurations and the states of the o band are dominated by one oblate configuration. In ^{98}Zr starting with spin $I^\pi = 6^+$ the states of the po(p) band indicate variable and sometimes strong mixing of prolate-deformed EXVAM solutions. The o band is built out of states dominated by oblate configurations, but particular spin states (10^+, 12^+, 14^+) manifest prolate mixing ($\sim$18%) since the oblate solution is very close in energy with a prolate-deformed one.

The relevant spherical occupations of the neutron and proton orbitals presented in Figs. 5 and 6 for the po(p) and o band in ^{96}Sr, respectively, and correspondingly in Figs. 7 and 8 for ^{98}Zr suggest changes in structure corroborated with the evolution of the shape mixing within these bands. Significant changes are found within the po(p) band at spin 10^+ and 16^+ in both nuclei.

The same evolution can be induced from the angular momentum alignment which indicates that maximum contribution in the direction of the total angular momentum is brought by $0h_{11/2}$ neutrons and $0g_{9/2}$ protons. The evolution of the structural changes is correlated with the faster alignment of the neutrons in $0h_{11/2}$ with respect to the protons in $0g_{9/2}$ within the po(p) band while similar alignment is manifested by the neutrons and protons occupying these orbitals along the o band in both nuclei. Nevertheless, the alignment along the po(p) band is specific for each nucleus. The particularities of the $I^\pi \geqslant 8^+$ states are reflected by the g-factor values that are larger in ^{96}Sr ($\simeq$0.24) with respect to the corresponding values in ^{98}Zr ($\simeq$0.14), both corroborated by the faster alignment of the valence neutrons occupying the $0h_{11/2}$ orbital. For the $I^\pi \geqslant 10^+$ states along the o band the g factors are slightly larger than 0.5 (0.44) in ^{96}Sr (^{98}Zr), supporting the role of the $0g_{9/2}$-proton alignment. In Figs. 1 and 2 are indicated by dashed-dotted lines some $M1$ transitions connecting states of the same spin. The strongest calculated strengths amount to $B(M1; 8_3^+ \to 8_1^+) = 1.292\mu_N^2$ in ^{96}Sr and $B(M1; 8_2^+ \to 8_1^+) = 1.600\mu_N^2$ in ^{98}Zr where the states are ordered according to the excitation energy.

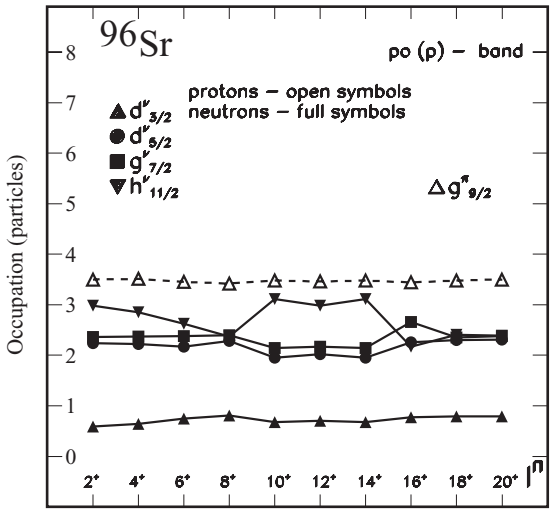

FIG. 5. Occupation of valence spherical orbitals for states of the po(p) band of ^{96}Sr.

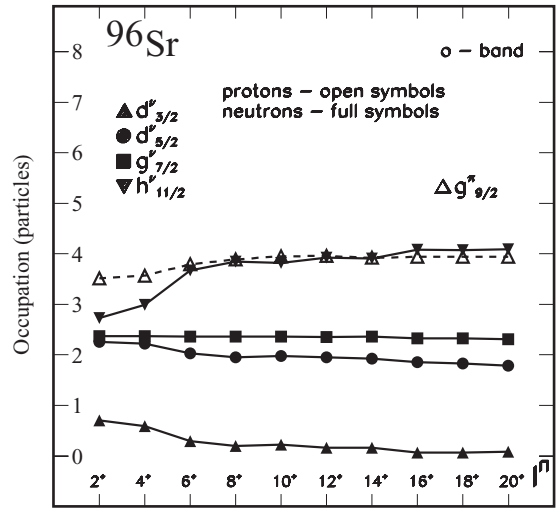

FIG. 6. The same as in Fig. 5, but for the o band of ^{96}Sr.

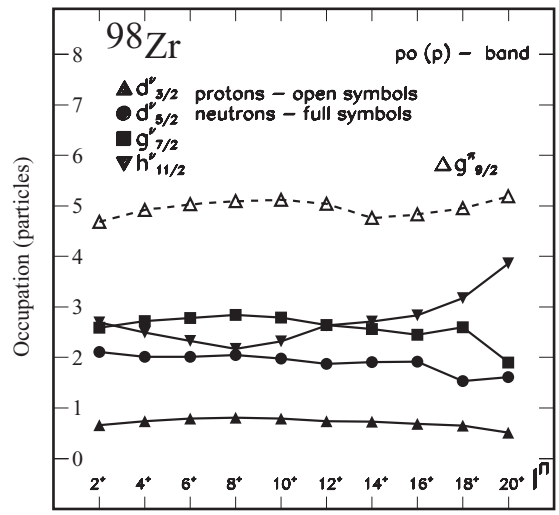

FIG. 7. Same as in Fig. 5, but for ^{98}Zr.

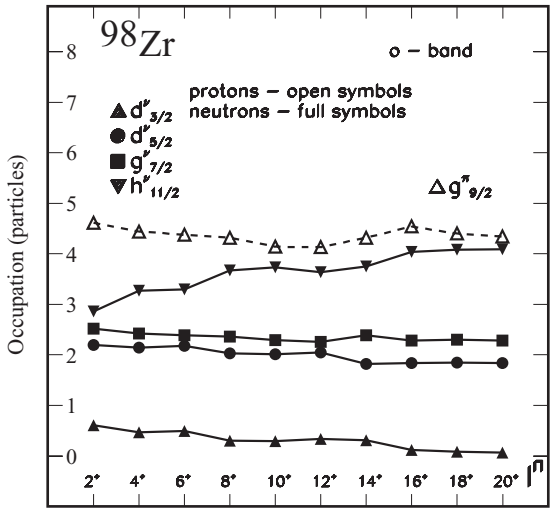

FIG. 8. Same as in Fig. 6, but for ^{98}Zr.

Lifetimes for the intermediate spin states in both nuclei have been measured [5]. By a simultaneous fit to several levels, assuming that they form a rotational band characterized by a common quadrupole moment, a value for Q_0 was estimated. The theoretical results indicate significant fragmentation of the $E2$ strength decaying to a given state due to the high density of states obtained at intermediate and high spins in both nuclei. In ^{96}Sr fitting the transitions in the $12^+ \to 10^+ \to 8^+$ cascade the reported value is $Q_0 = [220\,(15)]efm^2$ [5]. In ^{98}Zr the value $Q_0 = [200\,(10)]efm^2$ was estimated fitting the transitions in the cascade $12^+ \to 10^+ \to 8^+ \to 6^+$, but the highest considered transition could be a sidefeeding branch [5,8,9] indicated by the dotted line in the experimental spectrum in Fig. 2. For the measured cascade in ^{96}Sr the EXVAM results are in agreement with data: $B(E2; 12^+ \to 10^+) = 2332e^2fm^4$ and $B(E2; 10^+ \to 8^+) = [819\,(1329)]e^2fm^4$ for the left and right branch, respectively, in Fig. 1. In ^{98}Zr the theoretical strengths corresponding to the measured cascade are $B(E2; 12^+ \to 10^+) = 2300e^2fm^4$, $B(E2; 10^+ \to 8^+) = [719\,(1430)]e^2fm^4$ for the left and right branch, respectively, in Fig. 2, and $B(E2; 8_1^+(8_2^+) \to 6^+) = [1802\,(1034)]e^2fm^4$. The EXVAM spectroscopic quadrupole moments of the states building the discussed cascades are

$$Q^{\text{spec}}(8^+) = -120efm^2,$$
$$Q^{\text{spec}}(10^+) = -121efm^2,$$
$$Q^{\text{spec}}(12^+) = -124efm^2$$

in ^{96}Sr and

$$Q^{\text{spec}}(8^+) = -127efm^2,$$
$$Q^{\text{spec}}(10^+) = -130efm^2,$$
$$Q^{\text{spec}}(12^+) = -129efm^2$$

in ^{98}Zr. The corresponding quadrupole deformation parameter in both nuclei amounts to $\beta_2 \simeq 0.3$. The spectroscopic quadrupole moments of the states building the o band in both nuclei indicate smaller deformation for the underlying oblate configurations of the corresponding states. For the intermediate spin states we obtained

$$Q^{\text{spec}}(8^+) = 77efm^2,$$
$$Q^{\text{spec}}(10^+) = 94efm^2,$$
$$Q^{\text{spec}}(12^+) = 95efm^2$$

in ^{96}Sr corresponding to a variation of the β_2 between -0.19 and -0.23. In ^{98}Zr the calculated quadrupole moments

$$Q^{\text{spec}}(6^+) = 77efm^2,$$
$$Q^{\text{spec}}(8^+) = 71efm^2,$$
$$Q^{\text{spec}}(10^+) = 58efm^2,$$
$$Q^{\text{spec}}(12^+) = 56efm^2,$$

indicate smaller deformation. For comparison, the inferred deformation value for the 8^+ state is $\beta_2(8^+) = -0.17$. The decrease of the quadrupole moment values for the higher spins is connected with the mentioned prolate admixture in the structure of the corresponding wave functions.

IV. CONCLUSION

This work presents self-consistent results on the triple-shape coexistence specific for the 0^+ states and the evolution of the shape coexistence and mixing with increasing spin and excitation energy for the positive-parity states up to spin 20^+ in the $N = 58$ Sr and Zr isotopes within the *complex* excited VAMPIR model using a realistic effective interaction in a large model space.

The lowest four 0^+ states are described as a variable mixing of spherical, prolate, and oblate deformed excited VAMPIR configurations. The oblate-prolate mixing characterizes the low-spin states. At intermediate and high spins, prolate and oblate bands coexist in both nuclei. The comparison to the available data indicates qualitative agreement. The existing discrepancies with respect to the present data on some electromagnetic properties may be connected with the effective interaction and the dimension of the excited VAMPIR many-nucleon bases. To solve the remaining problems these studies will be extended to chains of neutron-rich isotopes in the $A \simeq 100$ region.

ACKNOWLEDGMENTS

This work has been supported by a grant of the Romanian National Authority for Scientific Research, CNCS – UEFISCDI, project number PN-II-ID-PCE-2011-3-0153.

[1] K. Kawade *et al.*, Z. Phys. A **304**, 293 (1982).
[2] H. Mach *et al.*, Nucl. Phys. A **523**, 197 (1991).
[3] G. Lhersonneau *et al.*, Phys. Rev. C **49**, 1379 (1994).
[4] J. H. Hamilton *et al.*, Prog. Part. Nucl. Phys. **35**, 635 (1995).
[5] W. Urban *et al.*, Nucl. Phys. A **689**, 605 (2001).
[6] P. Campbell *et al.*, Phys. Rev. Lett. **89**, 082501 (2002).
[7] H. L. Thayer *et al.*, J. Phys. G **29**, 2247 (2003).
[8] C. Y. Wu *et al.*, Phys. Rev. C **70**, 064312 (2004).

[9] G. S. Simpson *et al*., Phys. Rev. C **74**, 064308 (2006).
[10] E. Clément *et al*., CERN-INTC-2010-009/INTC-P-216-ADD-108/01/2010.
[11] J. Skalski, P.-H. Heenen, and P. Bonche, Nucl. Phys. A **559**, 221 (1993).
[12] J. Skalski, S. Mizutory, and W. Nazarewicz, Nucl. Phys. A **617**, 282 (1997).
[13] P. G. Reinhard, D. J. Dean, W. Nazarewicz, J. Dobaczewski, J. A. Maruhn, and M. R. Strayer, Phys. Rev. C **60**, 014316 (1999).
[14] A. Holt, T. Engeland, M. Hjorth-Jensen, and E. Osnes, Phys. Rev. C **61**, 064318 (2000).
[15] K. Sieja, F. Nowacki, K. Langanke, and G. Martínez-Pinedo, Phys. Rev. C **79**, 064310 (2009).
[16] Y.-X. Liu *et al*., Nucl. Phys. A **858**, 11 (2011).
[17] C. Özen and D. J. Dean, Phys. Rev. C **73**, 014302 (2006).
[18] J. E. García-Ramos *et al*., Eur. Phys. J. A **26**, 221 (2005).
[19] R. Rodríguez-Guzmán, P. Sarriguren, L. M. Robledo, and S. Perez-Martin, Phys. Lett. B **691**, 202 (2010).
[20] A. Petrovici, K. W. Schmid, and A. Faessler, J. Phys. **312**, 092051 (2011).
[21] A. Petrovici, K. W. Schmid, and A. Faessler, Prog. Part. Nucl. Phys. **66**, 287 (2011).
[22] J. Xiang *et al*., Nucl. Phys. A **873**, 1 (2012).
[23] E. Bender and K. W. Schmid, and A. Faessler, Nucl. Phys. A **596**, 1 (1995).
[24] L. K. Peker, Nucl. Data Sheets **68**, 165 (1993).
[25] B. Singh and Z. Hu, Nucl. Data Sheets **98**, 335 (2003).